J Forensic Sci, May 2003, Vol. 48, No. 3
Paper ID JFS2002303_483
Available online at: www.astm.org

John H. Wagner[1] *and Gordon M. Miskelly,*[1] *Ph.D.*

Background Correction in Forensic Photography I. Photography of Blood Under Conditions of Non-Uniform Illumination or Variable Substrate Color—Theoretical Aspects and Proof of Concept*

ABSTRACT: The combination of photographs taken at two or three wavelengths at and bracketing an absorbance peak indicative of a particular compound can lead to an image with enhanced visualization of the compound. This procedure works best for compounds with absorbance bands that are narrow compared with "average" chromophores. If necessary, the photographs can be taken with different exposure times to ensure that sufficient light from the substrate is detected at all three wavelengths. The combination of images is readily performed if the images are obtained with a digital camera and are then processed using an image processing program. Best results are obtained if linear images at the peak maximum, at a slightly shorter wavelength, and at a slightly longer wavelength are used. However, acceptable results can also be obtained under many conditions if non-linear photographs are used or if only two wavelengths (one of which is at the peak maximum) are combined. These latter conditions are more achievable by many "mid-range" digital cameras. Wavelength selection can either be by controlling the illumination (e.g., by using an alternate light source) or by use of narrow bandpass filters. The technique is illustrated using blood as the target analyte, using bands of light centered at 395, 415, and 435 nm. The extension of the method to detection of blood by fluorescence quenching is also described.

KEYWORDS: forensic science, photography, blood, background correction

Photography of crime scenes and forensic evidence consists of a well-developed suite of techniques that are able to provide graphic illustrations of many different types of evidence (1,2). However, the introduction of video and digital imaging has led to new possibilities in this field (3–5). Most forensic photographic techniques use combinations of lighting and camera angle to maximize the contrast between the evidence and any underlying substrate (1,2). Monochromatic light or narrow band pass light from lasers or alternate light sources, respectively, have provided significant increases in specificity of photographic reproduction or visual identification for certain types of evidence such as bloodstains and fingerprints (6,7). However, there are some circumstances where either non-uniform lighting of the surface of interest or patterning of the surface on which the evidence sits can lead to non-optimum visualization of the evidence in a given photograph. The non-uniform lighting may be a result of the lighting sources available or a result of the three-dimensional nature of the item being photographed. In addition, it is possible that the substrate is patterned with sufficiently strong colors that the evidence is not readily visualized or photographed. These problems can be reduced or eliminated by performing background corrections on photographic images.

The principle of the technique discussed in this paper is that while most colored compounds have broad absorptions in the visible region, with full widths at half maximum height (FWHM) in the range of 100 nm or more, some compounds have much narrower absorption bands. For example, blood contains hemoglobin, in which the iron porphyrin chromophore has an absorption band (the Soret band) centered near 415 nm with a FWHM of around 20 nm. This narrow bandwidth has been noted in a forensic context previously, leading Stoilovic to advocate the use of an alternate light source with a band centered at 415 nm for examination of blood evidence (7). However, if the substrate has variable absorbance at 415 nm, or is unevenly illuminated, the visualization of blood is made difficult even if a narrow-band light source is used.

An analogous problem exists in colorimetric analysis of solutions (e.g., blood or urine) for their concentrations of hemoglobin in the presence of other absorbing substances. The effect of the other absorbers can be eliminated by measuring the height of the narrow Soret band above an interpolation of the broad background absorbance. The simplest estimation of the background absorbance at the Soret wavelength is to measure the absorbance of the solution at wavelengths equidistant above and below the absorbance maximum and average these values. This procedure is referred to as an "Allen correction" in the clinical setting (8–11). Other wavelengths can also be used, with appropriate linear interpolation (10).

The application of background correction in image processing is well developed in astronomy and geographic remote sensing (where it is sometimes referred to as continuum correction) (12–14). The background estimation ranges from a simple linear interpolation to more complex curve-fitting of spectral data at many wavelengths. In both these fields, the light sources (stars, including the sun) are independent of the measurement device, and the detectors are scientific grade CCD detector arrays. Application of this concept to imaging with an artificial illuminant is less well developed. Background correction has also been applied to fluo-

[1] Forensic Science Programme, The Department of Chemistry, The University of Auckland, Private Bag 92019, Auckland, New Zealand.

* Research supported by funding from the University of Auckland, New Zealand.

Received 2 Sept. 2002; accepted 4 Jan. 2003; published 26 Mar. 2003.

rescence microscopy (15–17), although it has usually involved estimation of the background using data from a single additional wavelength.

This paper discusses applying a background correction technique to photographic images to provide increased discrimination, using bloodstain evidence as a particular example. The technique provides the possibility of locating additional possible bloodstain evidence beyond that identified visually or with standard forensic photography, without recourse to chemical enhancement. This has the advantage of reduction of the usage of potentially hazardous chemicals, particularly in the non-laboratory context, and is also advantageous if the bloodstain so located is to be used for subsequent analysis such as DNA typing.

Theory

The theory of the background correction method will first be developed in a quantitative manner for transmission mode photography, and will then be extended to approximate treatments of "normal" (reflectance) photography. The treatment is based on the use of a consumer digital camera that can provide linear images and that has controllable variable shutter speeds. Many high end consumer color digital cameras are able to export such linear images, often described as "RAW" images by manufacturers. Although we have used a color camera in our studies, the technique will work equally well for a linear monochromatic digital camera. Note that film cameras and standard processed digital images produce output where the image is approximately logarithmically related to light intensity, rather than linearly. Digital cameras operating in a linear mode provide values at each pixel that are proportional to both the intensity of the light incident on that pixel and the length of time of the exposure—i.e., they act as integrating detectors. The pixel values on a color digital camera are reported as red, green, and blue channels, each of which can have values from 0 (no light detected) to 255 (saturated). An "8-bit" camera or image only reports integer values within this range, while "10-bit" or "12-bit" cameras report values separated by 0.25 or 0.0625, respectively. The digital camera sensor itself responds to all visible wavelengths; common digital cameras use a grid of colored dyes to cause each pixel to respond to either red, green, or blue. The camera or computer software then interpolates this information to provide a value for red, green, and blue at each pixel. The dyes used to define the three channels have broad and overlapping responses; for example, the signals detected by a Canon D30 digital camera as a function of wavelength are shown in Fig. 1. The responses in this figure are not solely indicative of the sensitivity of the sensor array in that camera since they also contain contributions from the light source intensity (a xenon lamp), the monochromator used, and the camera lens. However, they do show that the red channel still responds to wavelengths in the blue region of the spectrum and vice versa. In our research only the values from the channel or channels that match best to the wavelength are used, since under most circumstances, the other channels will have a lower signal and therefore a higher relative amount of noise (vide infra). In this paper, the blue channel is used for most measurements since this channel has the greatest response near 415 nm. These considerations, obviously, would be unnecessary for a monochromatic camera.

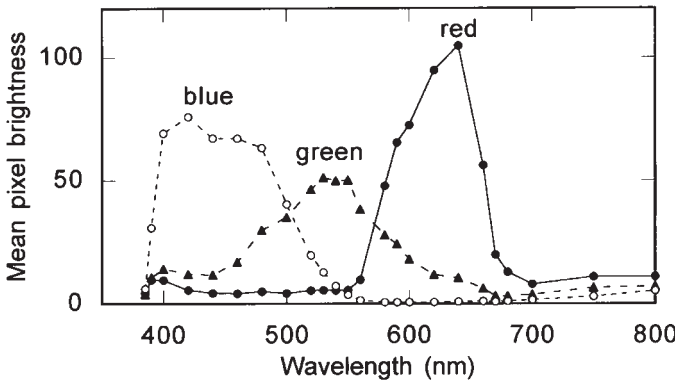

FIG. 1—*Uncorrected response function of the red, green, and blue sensors in a Canon D30 digital camera. Values were obtained by photographing a white card under constant camera settings while the illumination (the output from the excitation monochromator of a Hitachi F2000 fluorescence spectrophotometer, bandwidth 10 nm) was varied from 380 to 800 nm). Camera white balance was set at "flash".*

In transmission mode, the absorption of light by blood follows the Beer-Lambert law

$$A = \varepsilon\, c\, l \tag{1}$$

where c is the concentration of light absorbing substance, ε is the molar absorptivity (a quantity characteristic of a given light absorber at a given wavelength), l is the distance through which the light must pass, and A is the absorbance, defined as

$$A = \log_{10}\left(\frac{I_{\text{incident}}}{I_{\text{transmitted}}}\right) = \log_{10}\left(\frac{1}{\text{Transmittance}}\right) \tag{2}$$

where I_{incident} and $I_{\text{transmitted}}$ are the intensities of light incident on the substance and transmitted through the substance, respectively.

Digital Photography of Blood on a Homogeneous Surface under Uniform Illumination

In this section, we discuss optimum conditions given a digital camera that is able to provide a raw output of at least 10 bits in a linear mode, meaning that it should be able to discriminate 1024 levels of light in each channel.

If the surface on which the blood is deposited is evenly colored and the lighting is uniform, then the most optimal method for photographing blood will normally be to take a photograph using narrow bandwidth light at 415 nm or with a narrow bandwidth 415 nm filter on the camera (Note, however, that under some circumstances, the color of the substrate may lead to better discrimination using the visible absorption bands of hemoglobin near 550 nm or even further to the red.) The filter or source should have a bandwidth of 20 nm or less, although we have obtained satisfactory results with 50 nm wide light sources. The image should be as highly exposed as possible without getting saturation, while keeping the ratio

$$\text{signal to noise} = \frac{\text{difference between light intensity of bloodstain and of background}}{\text{variability of background in image}} \tag{3}$$

as high as possible. The variability of the image intensity due to the camera under these conditions will be determined by the noise of the detector pixels, and if this is determined by shot noise (with Poisson distribution) this noise will be proportional to the square root of the detected number of counts. The reason for the recommendation of high exposure is as follows: the more highly exposed a photograph is, the greater the average pixel value will be. Passage of light through a given amount of blood leads to a set absorbance at a given wavelength. Thus, a blood layer with an absorbance of 0.005 on a substrate will lead to a change from 200

to 198 if the average pixel level in the absence of blood is 200, but only a change from 50 to 49.5 if the average pixel level in the absence of blood is 50. (Note that on an 8-bit camera (256 levels) this latter change would be impossible to detect.) Having a "10-bit" or "12-bit" camera might suggest that blood stains corresponding to pixel changes of 0.25 or 0.0625, respectively, might be detectable. However, digital cameras tend to have some inherent variability between individual pixel responses and most surfaces are not completely uniform, so that a faint bloodstain will only be noticed if the pixel change is greater than the variability of the camera and greater than the variability in the substrate surface. The interpixel variability can be as large as ± 5 at an average level of 200 with the nominally 12-bit camera we have tested, although this value depends on the exact conditions of camera usage. If the photographer is willing to lose some spatial resolution by averaging pixels, the sensitivity can be increased due to the consequent reduction in interpixel variability (the decrease in variability being proportional to the square root of the number of pixels averaged). If the bloodstained region is less exposed, the light is non-uniform, or the substrate is patterned, then the detection limit will be increased from the ideal. There is an important caveat to this analysis: while nonlinear images from digital cameras have pixel values ranging from 0–255, the linear output from our particular camera saturates at a lower value—typically around 160 for the blue pixels (although this varies with camera settings). Thus it is either necessary to fully characterize the camera used or to bracket shutter speeds to ensure appropriate exposure.

When a photograph has been obtained under the optimal conditions for the homogeneous surface with uniform illumination, then contrast controls (or level controls in an image adjusting program such as Adobe Photoshop®) can be used to enhance the visibility of the image. This is no more image manipulation than altering the background (or zero) level and gain on a spectrophotometer.

Digital Photography of Blood on an Inhomogeneous Surface or under Non-Uniform Illumination—Transmission Mode

It is more likely that photography will be performed under conditions of non-uniform illumination, or blood will be on substrates that are not uniform in color. Natural wrinkles and folds of clothing or the three-dimensional nature of other casework exhibits can make it very difficult to have truly uniform lighting. Under these conditions it is possible to use pictures taken at wavelengths bracketing the absorbance maximum for blood to compensate for variations in the background or the light intensity.

As noted earlier, most absorptions in the visible region are broad, with widths in excess of 50–100 nm, while the hemoglobin in blood has a Soret band with a FWHM of about 20 nm. This difference in peak widths means that changes in absorption due to a variable background can be reduced or eliminated by applying a linear baseline correction using an appropriate choice of wavelengths, as shown in Fig. 2. As noted in the opening section of this paper, this baseline correction has already been reported for calculating hemoglobin concentrations in solution (8), and for analyzing specific absorption bands in remote sensing applications (12). The absorbance difference associated with the presence of blood is the height of B-D in the figure. This baseline correction will also compensate for a reasonable amount of variation in light intensity across the area being photographed. The three wavelengths used in this study were 395, 415, and 435 nm, with the outer two wavelengths being used to provide background correction for the 415 nm image. These outer two wavelengths are slightly closer to the Soret maximum than some previous authors have suggested for solution analyses (8,10). This is for two reasons: first, patterned substrates may well have color changes that would lead to additional spectral changes at longer wavelengths, and second, the throughput of light from a standard alternate light source that is detected by a standard digital camera falls off rapidly at wavelengths shorter than 400 nm. The decrease in light throughput also led us to develop a slightly different form of the absorbance equation than is usually given, so the full derivation is provided.

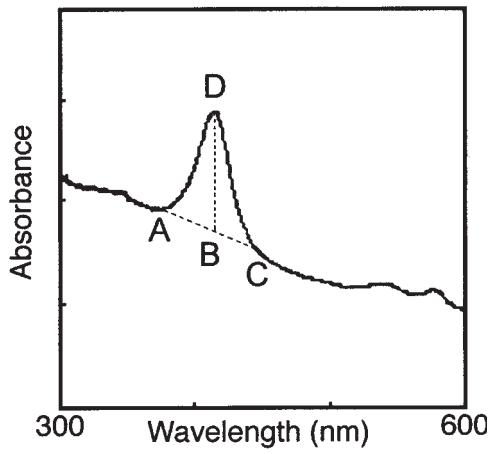

FIG. 2—*Diagram showing how background correction is performed for a narrow peak superimposed on a broad background. The distance BD will be proportional to the concentration of the compound corresponding to the narrow absorbance peak.*

For generality, let the wavelengths be λ_1, λ_2, and λ_3, where λ_2 is the wavelength most appropriate for the stain of interest and λ_1 and λ_3 are wavelengths equidistant above and below λ_2 (The equidistance constraint is readily removed by appropriate weighting as noted earlier (10), but leads to more complicated arithmetic.) Let the light intensity at wavelengths λ_1, λ_2, and λ_3 detected at the camera after passing through a non-absorbing substrate be $I_{i,1}$, $I_{i,2}$, and $I_{i,3}$, respectively. These detected light intensities will be controlled by the light source, the monochromator, any light-transmitting media (e.g., a light guide and/or any lenses or filters), and the camera response. Let the light intensity at wavelengths λ_1, λ_2, and λ_3 detected at the camera after passing through an absorbing substrate be $I_{t,1}$, $I_{t,2}$, and $I_{t,3}$, respectively. Linear digital cameras work as integrators, so the level at each pixel in a photograph will be directly proportional to both the light intensity falling on that pixel and the exposure time. Let the exposure times used at the three wavelengths be t_1, t_2, and t_3, respectively.

The Beer-Lambert law at a given wavelength λ_j can now be given in an integral form:

$$\text{Absorbance}_j = \varepsilon c l = \log_{10}\left(\frac{I_{i,j}t_j}{I_{t,j}t_j}\right) \tag{4}$$

If the background correction is taken as

$$\text{Background absorbance at } \lambda_2 = \frac{\text{Absorbance}_1 + \text{Absorbance}_3}{2} \tag{5}$$

then the corrected absorbance is

$$\text{Corrected absorbance at } \lambda_2 = \text{Absorbance}_2 - \frac{\text{Absorbance}_1 + \text{Absorbance}_3}{2} \tag{6}$$

Using the definition of absorbance at a given wavelength (Eq 4) this leads to

$$\text{Corrected absorbance at } \lambda_2 = \log_{10}\left(\frac{I_{i,2}t_2}{I_{t,2}t_2}\right) - \frac{1}{2}\left(\log_{10}\left(\frac{I_{i,1}t_1}{I_{t,1}t_1}\right) + \log_{10}\left(\frac{I_{i,3}t_3}{I_{t,3}t_3}\right)\right) = \log_{10}\left(\frac{I_{i,2}t_2}{\sqrt{I_{i,1}t_1 \cdot I_{i,3}t_3}}\right) + \log_{10}\left(\frac{\sqrt{I_{t,1}t_1 \cdot I_{t,3}t_3}}{I_{t,2}t_2}\right) \quad (7)$$

The first log term is a combination of ratios of the detected light at each wavelength when no absorption by the substrate is occurring, and is thus only a function of the instrumental set-up. Furthermore, if t_1, t_2, and t_3 are appropriately chosen then this term can be made very small. This can be done by choosing exposure times such that a neutral density image has been approximately equally exposed at each wavelength or by using exposure times such that $I_{i,2}t_2 = (I_{i,1}t_1 I_{i,3}t_3)^{1/2}$, either by prior calibration of the system with a uniform neutral density target or more simply by relying on the automatic exposure facility of the camera. This latter method works if it is assumed that the extent of the bloodstain is sufficiently small that it will not impact on the selection of exposure time and if the average spectral response of the substrate is comparatively constant over the wavelengths used. If necessary, the recorded images at each wavelength can be corrected by a multiplicative factor to allow for the fact that camera shutter speeds have discrete values that will not always be exactly appropriate. This multiplicative correction is aided by the inclusion of a uniform neutral density target of similar opacity to the substance of interest in the image. In addition, the relative exposure times can be monitored if the correct ratio of shutter speeds at the different wavelengths is known for the given light source—camera combination. We have found that incorporation of a standard is not usually necessary for qualitative detection of bloodstains with our system.

This then leaves the second log term in Eq 7. Standard image arithmetic programs only provide the four arithmetic operations of addition, subtraction, multiplication, and division. Therefore the geometric mean $\sqrt{I_{t,1}t_1 \cdot I_{t,3}t_3}$ is replaced with the arithmetic mean $(I_{t,1}t_1 + I_{t,3}t_3)/2$. This approximation is valid as long as $I_{t,1}t_1 \approx I_{t,3}t_3$ and this is true as long as the exposure times are chosen appropriately as suggested above and as long as the substrate absorbance at any given point is not changing too rapidly over the wavelength range 435–395 nm. This leads to the approximate equation

$$\text{Corrected absorbance at } \lambda_2 \approx \log_{10}\left(\frac{I_{t,1}t_1 + I_{t,3}t_3}{2\,I_{t,2}t_2}\right) \quad (8)$$

In practice we do not proceed this far, but rather use the related transmittance equation

$$\text{Corrected transmittance at } \lambda_2 \approx \frac{2\,I_{t,2}t_2}{I_{t,1}t_1 + I_{t,3}t_3} \quad (9)$$

both because it avoids the need to perform a logarithmic transformation and because it leads to blood looking darker than the substrate (which is what crime scene investigators are used to observing). However, if desired, an approximate logarithmic transformation can be performed using an appropriate mapping transform for pixel intensity (In Adobe Photoshop®, this can be performed using the "Curves" instruction together with an appropriate transformation curve.)

Digital Photography of Blood on an Inhomogeneous Surface or under Non-uniform Illumination–Reflectance Mode

If the reflectance measurement is from a non-scattering substrate, then the treatment is identical to the above transmittance discussion, with the appropriate replacement of transmitted light by reflected light.

$$\text{Corrected reflectance at } \lambda_2 \approx \frac{2\,I_{r,2}t_2}{I_{r,1}t_1 + I_{r,3}t_3} \quad (10)$$

where I_{rj} is the detected reflected light intensity at wavelength j.

For the more common situation where the reflected light is subjected to scattering as well as reflection there are several options. The easiest one (and the one most appropriate for non-quantitative inspection for potential bloodstains) is to ignore scattering effects and use Eq 10. This approach has been used in remote sensing applications, with the negative logarithm of the corrected reflectance as calculated by Eq 10 being referred to as the "apparent absorbance" (12). It has also been used for other quantitations using reflectance data, with phenomenological, rather than theoretical, justification (18,19). This equation is only an approximate treatment, and in particular, breaks down when specular reflection is significant.

An alternative is to use the Kubelka-Munck treatment for diffuse reflectance, assuming that most scattering is occurring from the substrate (20,21). The treatment described below involves extending the Kubelka-Munck theory into a range of reflectances where it does not hold quantitatively without the incorporation of additional factors (such as use of Fresnel coefficients) (20,21). However, the equation derived from this treatment can still be used in a qualitative manner. The simplified Kubelka-Munck treatment gives two equations

$$\left(\frac{K}{S}\right)_j = \frac{(1 - R_j)^2}{2R_j} \quad (11)$$

and

$$\left(\frac{K}{S}\right)_j = \left(\frac{k}{s}\right)_{\text{substrate},j} + c_{\text{analyte}}\left(\frac{k}{s}\right)_{\text{analyte},j} \quad (12)$$

where R_j is the observed reflectance at a given wavelength, $(K/S)_j$ is the ratio of absorption to scattering at that wavelength, and the k/s terms are the individual contributions to the K/S ratio from the substrate and the analyte (with concentration c_{analyte}). Equation 12 shows that K/S is linearly related to the concentration of a given absorbing species (in the present case, blood). These equations can be applied to the analysis of blood stains by using K/S values at wavelengths 1 and 3 to estimate a value of K/S at wavelength 2 in the absence of blood, giving the following equation

$$\left(\frac{K}{S}\right)_2 = \frac{1}{2}\left(\left(\frac{K}{S}\right)_1 + \left(\frac{K}{S}\right)_3\right) + c_{\text{analyte}}\left(\frac{k}{s}\right)_{\text{analyte},2} \quad (13)$$

and therefore

$$\text{corrected } \frac{K}{S} \text{ at wavelength 2} = \left(\frac{K}{S}\right)_2 - \frac{1}{2}\left(\left(\frac{K}{S}\right)_1 + \left(\frac{K}{S}\right)_3\right) = c_{\text{analyte}}\left(\frac{k}{s}\right)_{\text{analyte},2} \quad (14)$$

Production of an image using this equation would require considerable mathematical manipulation of the original three images, so a simplified version is suggested below. If the observed reflectance

$\ll 1$ (valid for many casework samples) then

$$(1 - R_j)^2 \approx 1 - 2R_j \tag{15}$$

and

$$\left(\frac{K}{S}\right)_j \approx \frac{(1 - 2R_j)}{2R_j} = \frac{1}{2R_j} - 1 \tag{16}$$

and therefore

$$\text{corrected } \frac{K}{S} \text{ at wavelength 2} \approx \left(\frac{1}{2R_2} - 1\right) - \frac{1}{2}\left(\left(\frac{1}{2R_1} - 1\right) + \left(\frac{1}{2R_3} - 1\right)\right) \approx \frac{1}{2R_2} - \frac{1}{2}\left(\frac{1}{2R_1} + \frac{1}{2R_3}\right) \tag{17}$$

Thus an image calculated using

$$\text{pixel level in image} \approx \text{constant} * \left(\frac{1}{R_2} - \frac{1}{2}\left(\frac{1}{R_1} + \frac{1}{R_3}\right)\right) \tag{18}$$

should have pixel levels proportional to the amount of blood at each point. Once again this equation can be adapted for use with a digital camera. If we select the exposure times such that $I_{\text{rstd},1}t_1 = I_{\text{rstd},2}t_2 = I_{\text{rstd},3}t_3$ where $I_{\text{rstd},j}$ is the detected reflected intensity from a neutral density standard at wavelength λ_j and t_j is the exposure time used at wavelength λ_j and furthermore, if we approximate that at all points $(I_{r,1}t_1 + I_{r,3}t_3)/2$ is directly proportional to $I_{\text{rstd},j}t_j$, then the above equation can be rewritten as

$$\text{pixel level} \approx A * \left(\frac{(I_{r,1}t_1 + I_{r,3}t_3)}{I_{r,2}t_2} - \frac{1}{2}\left(\frac{(I_{r,1}t_1 + I_{r,3}t_3)}{I_{r,1}t_1} + \frac{(I_{r,1}t_1 + I_{r,3}t_3)}{I_{r,3}t_3}\right)\right) \approx B * \text{concentration} \tag{19}$$

where $I_{r,j}$ is the detected light intensity at wavelength λ_j. The constant A is chosen so that the resulting pixel levels range from 0 to approximately 200. As written this equation will lead to blood appearing as bright spots on a dark background—images processed in this manner can then have their brightness levels inverted so that blood appears dark. Since this equation requires more mathematical calculations than the earlier treatment represented by Eq 10 we have used Eq 10 in almost all of our photographic studies. This decision has precedent, since as noted earlier, many other authors have also chosen to use phenomenological equations relating concentration and reflectance from scattering substrates rather than physically-derived equations, even when performing quantitative measurements. It should be noted that if the right-hand side of Eq 10 is inverted, it corresponds to the first term in Eq 19, so that the second term in Eq 19 can be regarded as a correction factor. We have examined whether this is a valid correction factor on a few patterned substrates, and find that it does sometimes lead to improved removal of the background pattern.

Non-linear Images

Most digital cameras simulate traditional photography by supplying images in a "non-linear" format. The camera sensors still act in a linear mode, but their information is processed in the camera or by the computer software to provide an image where increments in pixel brightness are linearly related to optical density rather than light intensity. Thus, the images are approximately logarithmic in light intensity. Such images can also be treated to background correction, but the correction is now done by *subtraction* of the estimated background image (i.e., the average of the 395 and 435 nm images) from the 415 nm image.

$$\text{Corrected apparent absorbance at } \lambda_2 \approx \log(I_{r,2}t_2) - \frac{\log(I_{r,1}t_1) + \log(I_{r,3}t_3)}{2} \tag{20}$$

If the "non-linear" transformation was exactly logarithmic and the camera and software had adequate resolution, this should lead to identical results to division of the linear images. In practice, subtraction of the non-linear images does not give as good results as division of the linear images, suggesting either that the transformation is not exactly logarithmic or that some intensity information is lost in the transformation. This is particularly true if the image is "8-bit". Furthermore, if non-linear imaging is to be used, photographs should be exposed to give pixel brightnesses on the background substrate in the "mid-range" (i.e., the auto-exposure setting is often close to the ideal) as opposed to the earlier suggestion that for *linear* images an image may be better to be slightly overexposed compared with the autoexposure setting (as long as no pixels in the region of interest are saturated).

Experimental

The camera used was a Canon D-30 digital single lens reflex camera, with either a Canon 24-85 mm zoom lens or a Canon EF 100 mm F2.8 mm macro USM lens attached. This camera has a CMOS detector with 2160 × 1440 active pixels for a total of 3.11 M pixels. The camera was mounted on a camera stand or tripod and was activated from a computer using the programs Remote Capture (Canon) or D30Remote (Breeze Systems) to avoid camera motion and thereby ensure registry of the images. Photographs were taken in a black box or in a dark room. The camera was manually focused, the aperture was set at its maximum, and the camera was then either set on automatic shutter speed or the shutter was set based on earlier calibrations. The ISO setting was either 200 or 400. In some photographs a "50%" grey card (18% reflectance compared with a standard white) was used as a standard. A cap was placed over the viewfinder after the lens had been focused to prevent inaccuracies in the exposure calculation. This was particularly important for the 395 nm photographs due to the low detected light intensity at this wavelength.

The detected light intensity using the Polilight—Canon D-30 combination decreased by approximately 100 times from 435 to 395 nm, so variable shutter speeds were used to obtain similar integrated light levels for each photograph (see companion paper for justification of this approach). Substrates were chosen to represent a range of possible fabrics, colors, and patterns. Bovine blood obtained from a local abattoir was preserved with 0.2% w/v EDTA and stored at 4°C. Possible bloodstains on the casework clothing were tested with Combur^3-Test® E test strips (Roche). The files (RAW format) were either transferred directly to the computer using the above-mentioned programs or saved onto a 64 MB card in the camera and then transferred to the computer using the Canon program ZoomBrowser. The raw files so obtained are in a proprietary 12 bit linear format. These were then converted into 16 bit TIFF files using Canon ZoomBrowser, with the conversion set to linear mode and with the white balance set to "flash" or "cloudy" (these appeared to be the closest white balance settings to the white light of our Polilight).

The light source used was a Rofin Polilight alternate light source, which consists of a xenon lamp, narrow bandpass filters,

and a liquid light guide with a glass collimator lens. The filters have nominal bandwidths varying from 40–80 nm, although our particular instrument now has slightly degraded performance compared to the original specifications. The most appropriate settings for obtaining light centered around 395, 415, and 435 nm were determined by monitoring the Polilight output with a laboratory spectrophotometer as the internal filters were fine tuned. For some of the early characterization, experiments, the light exiting from the excitation monochromator of a Hitachi F2000 fluorescence spectrophotometer was used. This light had a bandwidth of 20 nm. Characterization of filter transmission, Rofin Polilight output, and substrate reflectivity was performed using an S2000 Ocean Optics fiber optic spectrophotometer.

The TIFF files obtained were combined mathematically using the filters in Fovea Pro 2.0 (Reindeer Graphics) installed in Photoshop 6.0 (Adobe Systems). The 395 and 435 nm photographs were averaged, and then the 415 nm photograph was divided by the average result. This corresponds to Eq 10 in the theory section. The program performs both mathematical calculations separately for each channel (red, green, and blue) at each pixel. To ensure that the final image has a spread of values within the range 0–255 the division of the images was usually followed by a mathematical transformation (Fovea Pro allows this to be done as part of the image mathematics process, to prevent loss of image information). For example, a division of the processed image by 0.005 followed by a subtraction of 128 would cause the following: If the 415 nm image is identical to the average of the 395 and 435 nm images, the image division should lead to an initial value of 1, which would then become 72 after the calculation. Therefore, given random noise in each photograph the processing should lead to a narrow range of pixel brightnesses centered at 72. If greater absorption occurs in the 415 nm photograph than predicted from the average of the 415 and 395 nm photographs, then this will lead to a value significantly less than 72, and vice versa. The final step was to use the Levels control in Adobe Photoshop to expand the calculated levels to use the full range of 0–255 levels. This would not be necessary for machine detection, but is necessary for human interpretation of the images as a result of the human eye's inability to see small differences in shades of grey. The transmission mode images used to test the linearity of the camera and applicability of Eq 9 were not subjected to levels adjustment and instead the image division was followed by a division by 0.005 to obtain pixel levels spread over the brightness scale.

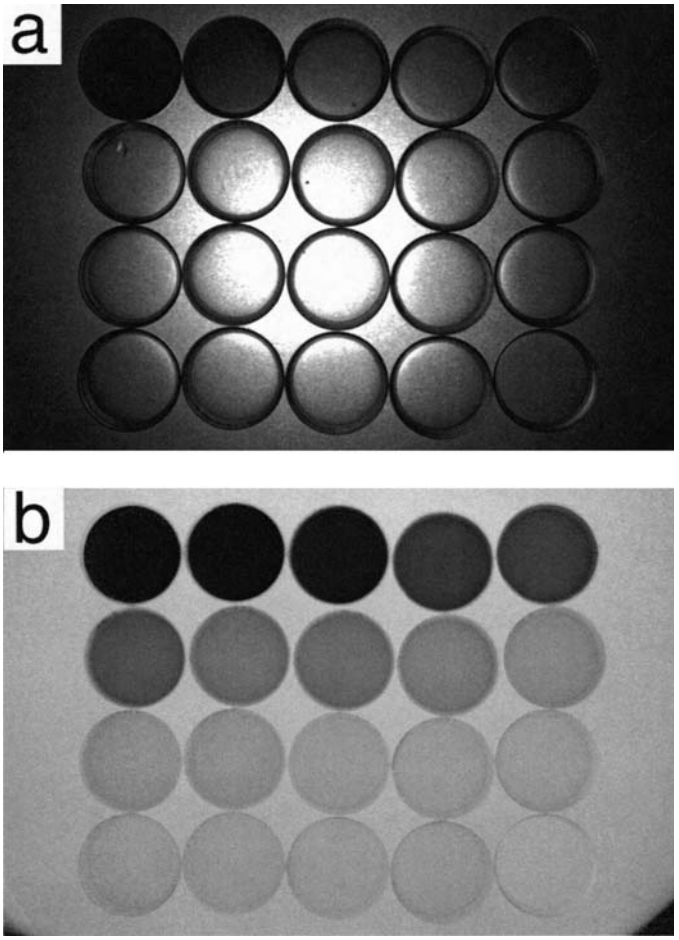

FIG. 3—*Photographs (in transmission mode) of petri dishes filled with diluted blood (nominal depth 5 mm).* a) *Image taken with 415 nm light from a Polilight. The image has had the pixel levels adjusted for optimum contrast.* b) *Image obtained by processing images taken at 395, 415, and 435 nm using Eq 9 then multiplying all pixels by 200. The solutions are bovine blood diluted as follows: top row, left to right 50–400 times, 2nd row 600–1500 times, 3rd row: 2000–3500 times, bottom row 4000–5000 times, with water at bottom right.*

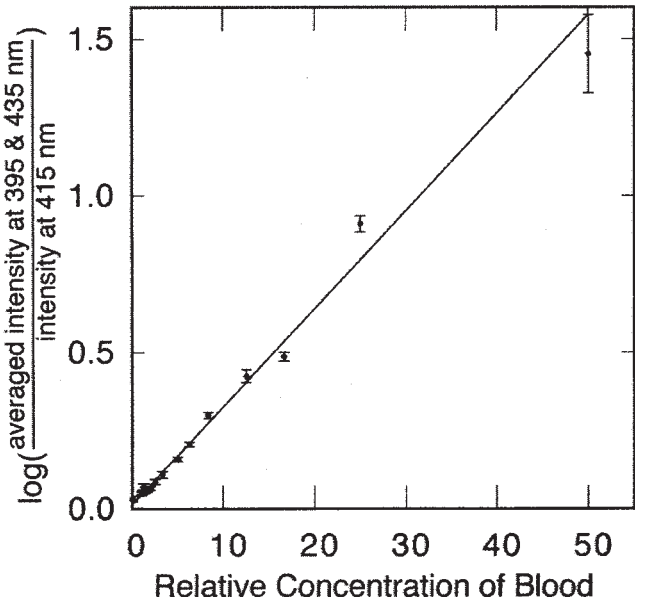

FIG. 4—*Graph showing the logarithm of the ratio (average brightness of the 395 and 435 nm images in the center of each petri dish)/(average pixel brightness of the 415 nm image in the center of each blood-filled petri dish) in image 3*b *vs the relative concentration of blood in the petri dishes. The line is a weighted least squares fit with each weight being proportional to the reciprocal of the square of the relative standard deviation of the pixel brightnesses in the center of each petri dish in Fig. 3*b.

Results

This paper focuses on general aspects of this image analysis technique, and application of the three Eqs 9 (transmission), 10 (reflection), and 19 (diffuse reflection). Specific experimental issues will be dealt with in a subsequent paper. Figure 3 shows a photograph of petri dishes containing blood solutions taken using transmitted light at 415 nm, together with the image corresponding to the transformation in Eq 9 applied to photographs taken with illu-

mination centred at 395, 415, and 435 nm, respectively. It should be noted that blood does absorb to some extent at all three wavelengths, but that it is significantly more absorbing at 415 nm. The original images at all wavelengths show effects of non-uniform lighting due to the limited size of the illumination source (see for example Fig. 3*a*). The processed image (Fig. 3*b*) shows little or no effects due to the non-uniform lighting. The difference in intensity near the edge of each petri dish is due to the meniscus affecting the solution depth. Figure 4 shows a plot of the logarithm of the ratio of the mean pixel level in the middle of each petri dish (as obtained by averaging the 395 and 435 nm images) to the mean pixel level of the same region in the 415 nm image versus the relative blood concentration. The line shown is a weighted least squares fit allowing for the slight difference in pixel variability as the brightness increases (the weights used were the squares of the reciprocal of the estimated relative standard deviation, fitting the noise in the observed data to an equation of the form noise = A + B*(brightness level)$^{1/2}$. The figure shows that the camera can behave in a quantitative manner under these conditions over a reasonable concentration range. However, this technique is more appropriate for qualitative or at best semi-quantitative identifications of bloodstains and that is the focus of the remaining experiments reported here.

Figure 5 shows a 415 nm photograph: (a) and a three-wavelength processed photograph, (b) of a strongly patterned piece of cloth, this time obtained by reflectance imaging under more uniform lighting conditions. The numbers in the images are bloodstains, with the numerical value representing the dilution of the blood prior to application. Note that the processed image has a greatly reduced background pattern relative to the intensity of the blood stain. Figure 5*c* shows this same image treated using the simplified Kubelka-Munck transformation given in Eq 19. In this instance the intensity differences in the pattern in the image are greatly reduced by the treatment of Eq 19 leading to a slightly better definition of the blood especially for the twenty-fold dilution. Figures 5*d* through *f* show the results obtained by using only two wavelengths (415 nm with background estimated using 435 nm) in linear mode, using three wavelengths in non-linear mode (the "normal option" with a digital camera), and using only two wavelengths in non-linear mode, respectively. While

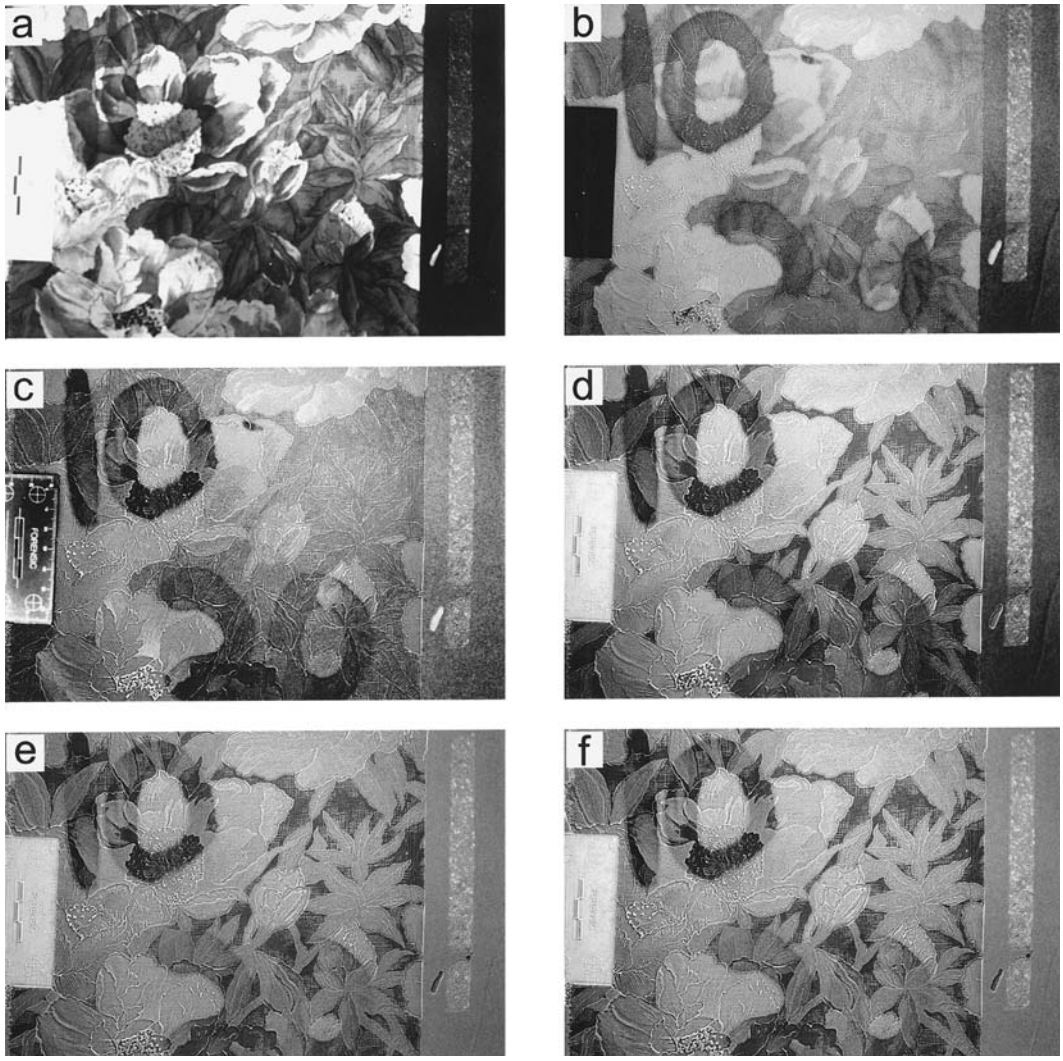

FIG. 5—*Photographs of patterned cloth with blood stains at 10-fold and 20-fold dilution (as shown by the numerals). Pattern included orange, white, blue, and green, with some weak fluorescence.* a) *Image taken with 415 nm light from a Polilight.* b) *Image obtained by processing images taken at 395, 415, and 435 nm using Eq 10.* c) *Image obtained by processing images taken at 395, 415, and 435 nm using Eq 19.* d) *Image obtained by ratioing images at 415 nm and 435 nm.* e) *Image obtained by subtracting non-linear images according to Eq 20.* f) *Image obtained by subtracting image at 435 nm from that at 415 nm. All images have had the pixel levels adjusted for optimum contrast.*

these last three images provide better discrimination of the blood from the pattern than does the 415 nm image (Fig. 5*a*), they do not provide as good background removal as the three-wavelength linear processed images (Fig. 5*b* and *c*).

This background correction technique should be appropriate for the photography of blood on any substrate that does not have a sharp peak or valley in absorbance near 420 nm. Given that this technique is non-destructive, it can be attempted after single wavelength examination for bloodstains. If no additional stains are evident, the item can then be enhanced chemically, and the enhanced stain examined normally or again by this technique, using the appropriate wavelengths for the enhancing agent used. We have only observed one problematic substrate so far—a brown/red carpet fragment. Processing of images taken at 395, 415, and 435 nm using Eq 10 led to a processed image in which the blood was either indistinguishable from the background or was even lighter than the background. This latter effect was almost certainly due to specular reflection from the blood surface. Two strategies were used to visualize blood on this substrate: First, the substrate was photographed under 650 nm light with the result shown in Fig. 6*a*. Second, since it had been noticed that the carpet showed weak red fluorescence when irradiated with blue light a long pass filter (>550 nm) was placed on the camera, photographs were taken while the carpet was illuminated with light at 395, 415, and 435 nm, and the red channel of the obtained images were processed according to Eq 10 to give Fig. 6*c*. In comparison, Fig. 6*b* is the fluorescence image obtained without the background correction using illumination at 415 nm and the longpass filter, showing much greater background variation than the processed image. It should be noted that other red-brown fabrics have performed well using the standard background correction technique, so that the problems encountered in absorbance mode photography were due to the specific dyes in this piece of carpet.

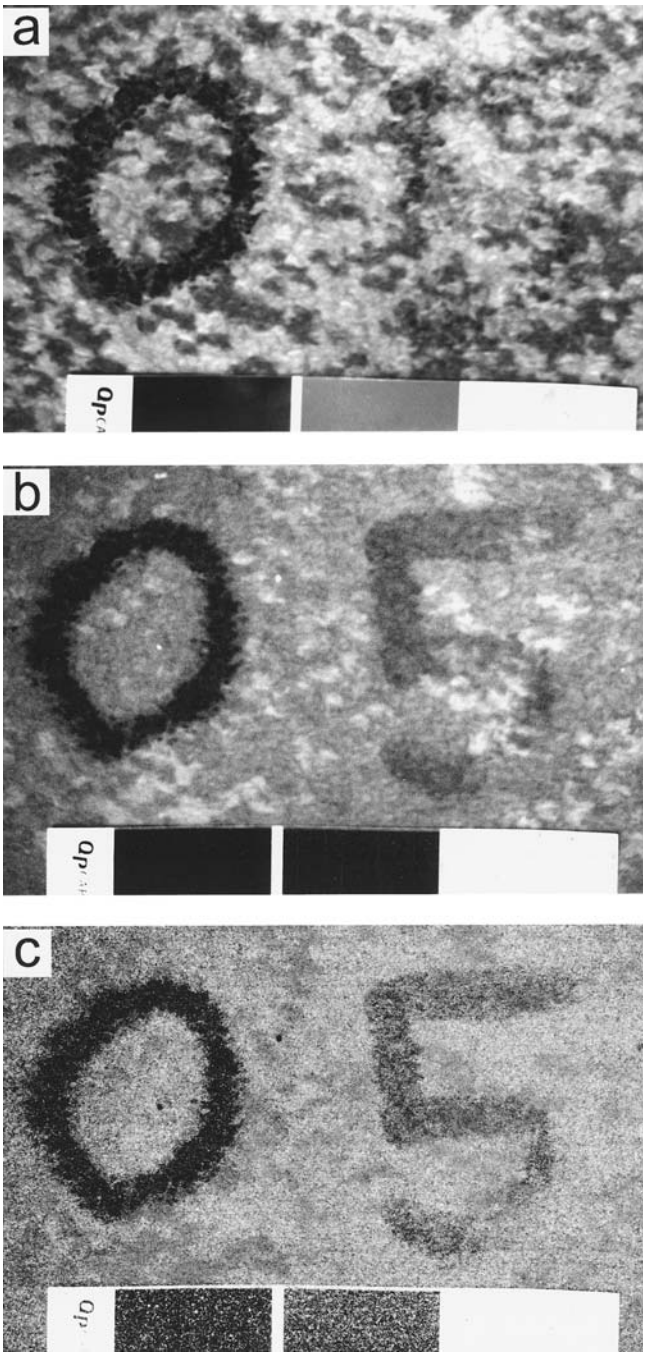

FIG. 6—*Images of a red-brown carpet fragment with undiluted ("0") and 5-fold diluted ("5") blood stains.* a) *Image taken at 650 nm.* b) *Fluorescence mode image taken by illuminating carpet at 415 nm and photographing through a long pass filter (>550 nm).* c) *Image obtained by combining fluorescence mode images taken by illuminating carpet at 395, 415, and 435 nm and photographing through a long pass filter, using Eq 10. All images have had the pixel levels adjusted for optimum contrast.*

Case Examples

Three examples of difficult substrates from casework were examined to evaluate the usefulness of this technique.

Case 1: Dark red rumpled shirt with glossy finish—The rumpled nature and glossy finish of the garment made it very difficult to detect blood on this shirt by eye using a bright white light or a narrow bandwidth blue light. Although the three wavelength technique using the light from a Polilight lightguide made it considerably easier to see suspected patches of blood compared with a visual examination under either white or blue light, it did not completely remove the effect of the specular reflectivity of the fabric. It is possible that diffuse lighting would have provided a better final result. The multiwavelength technique readily lead to the location of all the blood which had been located by a manual search (one of these areas is marked as a white rectangle in Fig. 7*a*). In addition, blood on the lower part of the shirt was also detected. Of interest (Fig. 7*b*) is the arrowed area corresponding to the white rectangle in Fig. 7*a*, which shows where the forensic technician had used a moistened Combur® stick to test a patch of blood. This rubbing pattern could not be observed visually, with only the two darker patches in the area being visible to the naked eye.

Case 2: Dark blue stretch jeans—These jeans had some obvious bloodstains which had been located by visual forensic examination (shown marked with white rectangles in Fig. 8*a*). The photographs at each wavelength were taken with exposure settings such that the blue channel of the pixels representing the dark blue jeans had average brightness levels of 50–60 in the linear photographs. The three wavelength background correction technique using the linear images (Fig. 8*b*) showed additional, paler areas of staining, selected regions of which were tested with Combur® sticks with results that supported the stains being blood. The photographs of these jeans were also analyzed by the two wavelength (415 and 435 nm) background correction method using ratios of linear images (Fig. 8*c*) and differences of non-linear images (Fig. 8*e*). Analysis

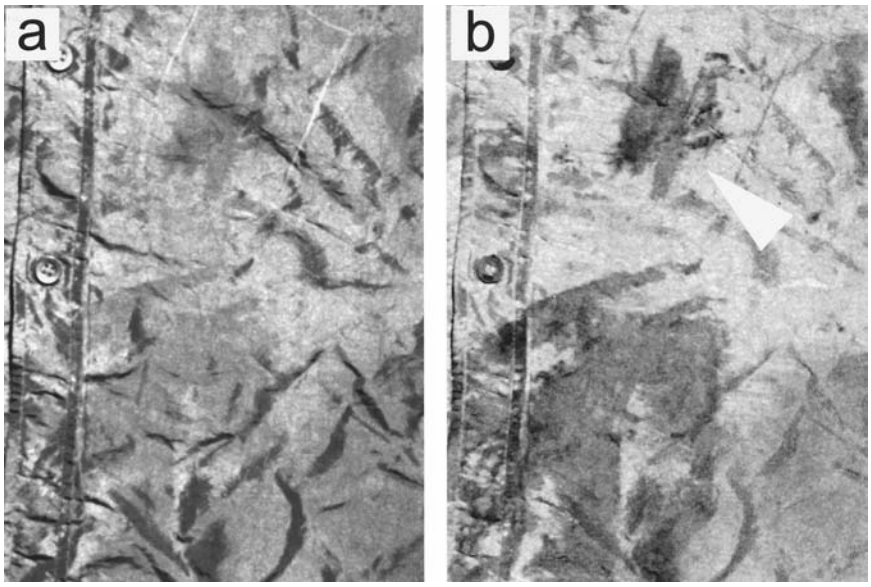

FIG. 7—*Portion of image of dark red crumpled glossy shirt.* a) *Image taken at 415 nm.* b) *Processed three wavelength image. Note area (arrowed in image* b*) where application of moistened Combur® stick has spread blood from the initial stains (darker spots within rubbing pattern). Both images have had the pixel levels adjusted for optimum contrast.*

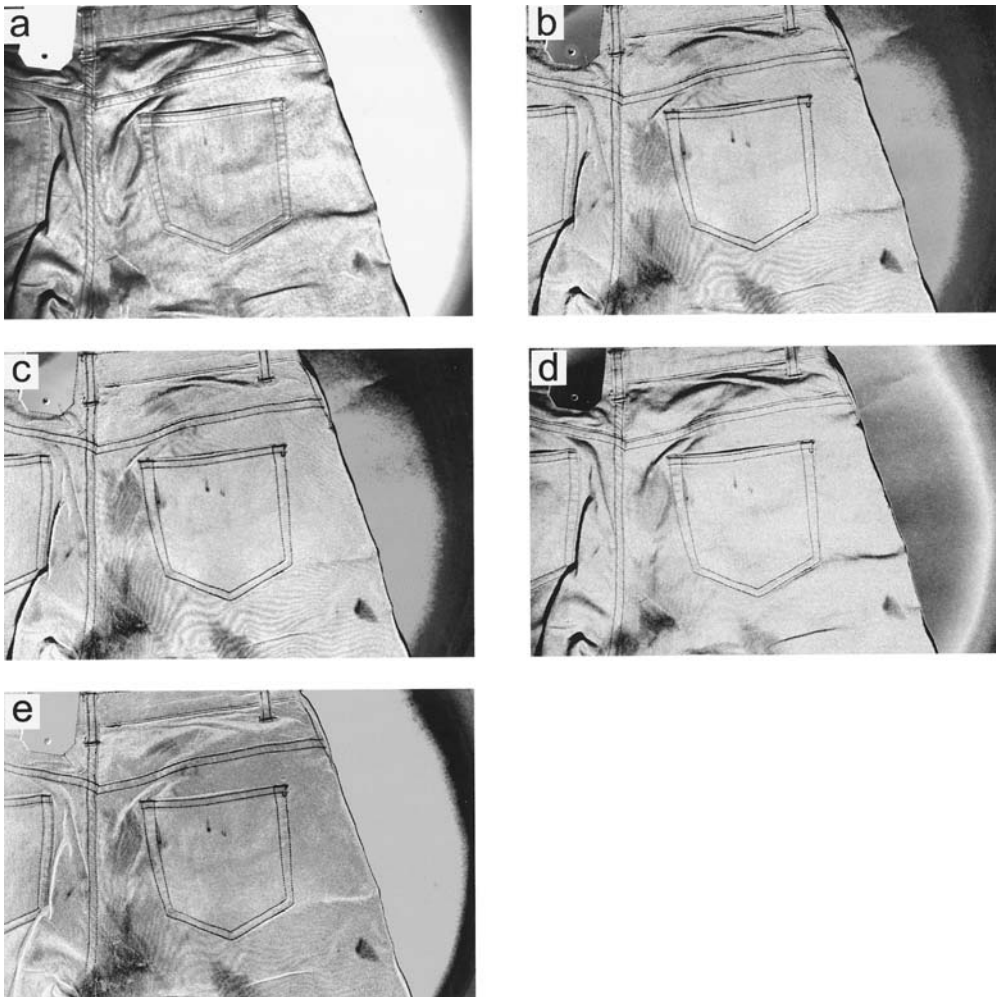

FIG. 8—*Images of bloodstained dark blue jeans, illustrating effects of different image processing.* a) *Image taken with 415 nm light from a Polilight.* b) *Image obtained by processing images taken at 395, 415, and 435 nm using Eq 10.* c) *Image obtained by ratioing images at 415 nm and 435 nm.* d) *Image obtained by subtracting non-linear images according to Eq 20.* e) *Image obtained by subtracting image at 435 nm from that at 415 nm. All images have had the pixel levels adjusted for optimum contrast.*

of the three photographs obtained at 395, 415, and 435 nm using differences of nonlinear images according to Eq 20 gave the image shown in Fig. 8*d*. It is seen that all processed images are able to detect the darker bloodstains, but the non-linear methods do not as readily enhance some of the fainter blood staining. All of the images in Fig. 8 show Moire patterns on the jeans, presumably due to interaction of the camera pixel grid and the regular weave of the fabric. The Moire patterning is enhanced in the division of the linear images. This effect is observed on many fabrics with well-defined weaves but does not appear to significantly affect detection of bloodstains.

Case 3: Black jeans with blood and dirt—These black jeans were covered with dust of a similar apparent color to blood (under white light illumination), and visual analysis under white light had not been able to locate any blood stains. Furthermore, Combur® testing showed that there was weak peroxidase-like reactivity over most of the jeans, indicative of blood dust or transfer of trace blood at the scene or in the packaging used for the item. This meant that it would be difficult to ascertain the positions of faint bloodstains by chemical enhancement. Photographic imaging of the front of the jeans using illumination centered at 395, 415, and 435 nm followed by processing equivalent to Eq 10 to reduce background variations led to an image that showed a dark area on the jean fly, and a lighter stain beneath the right pocket (both arrowed in Fig. 9*b*). Combur® stick testing of both these areas gave a significantly stronger response indicative of blood than did randomly selected areas of the jeans. Again, banding due to Moire effects can be observed in the processed image.

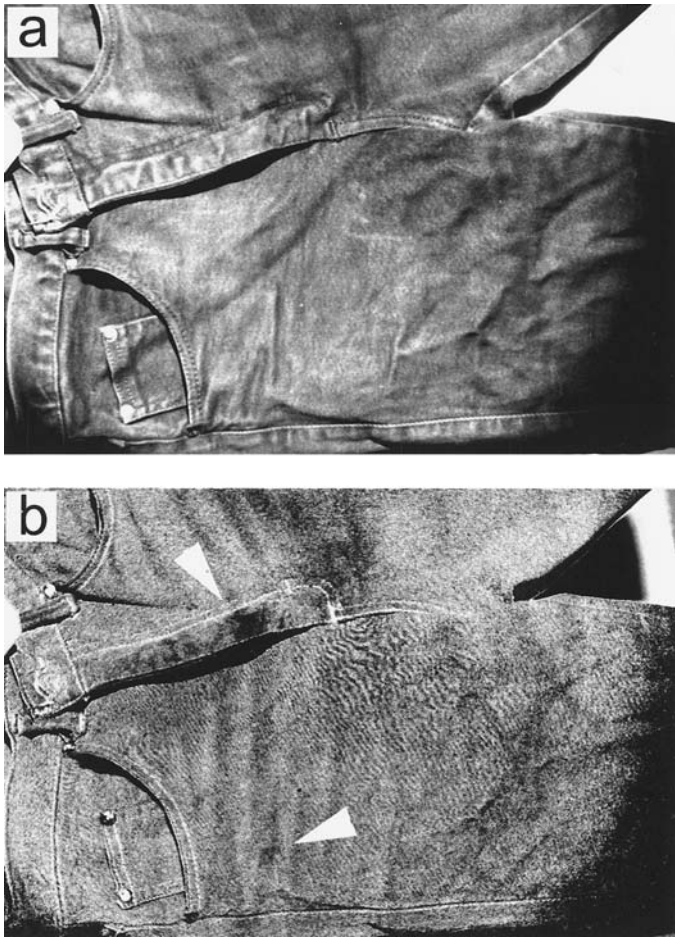

FIG. 9—*Images of bloodstained black jeans which were covered in red-brown dirt.* a) *Image taken with 415 nm light from a Polilight.* b) *Image obtained by processing images taken at 395, 415, and 435 nm using Eq 10. Both images have had the pixel levels adjusted for optimum contrast. Note the bloodstains on the fly and near the pocket (arrowed), neither of which were visible to the naked eye but both of which tested positive for blood using moistened Combur® sticks.*

Discussion

The three wavelength processing of the linear photographic images clearly leads to improved detectability of blood on patterned substrates and under conditions where the substrate color or the illumination level change. The enhancement is obtained without the use of chemical sprays and it is non-destructive, so that it can be an option where blood staining is suspected but is not readily detected by eye. The nonchemical nature of the technique also means that it can be used on substrates such as historical artifacts where chemical enhancement might be inappropriate, and more generally it could lead to reduced use of enhancement chemicals at crime scenes. The absolute sensitivity of this method is obviously nowhere near that of the catalytic reagents such as luminol or leuco dyes, but often that high sensitivity is not needed at a crime scene—rather it is the selectivity and discrimination from the substrate which is more important.

All the photographic images in this paper except Fig. 6 have used an alternate light source to select appropriate regions of the visible spectrum, with no filters on the camera. This requires that the photography be performed in a darkened area to prevent stray light affecting the images. Photography can also be performed using narrow bandpass filters on the camera, in which case the area does not have to have to be darkened—a technique already used when single monochromatic photographs are to be made (7). However, combination of photographs taken with different filters (or with and without filters) can lead to slight misregistration between images that causes the processed image to have a slightly "three-dimensional" appearance and a worse detection limit for blood due to incomplete removal of the edges of background patterns. This effect can be reduced by moving the images into better registration with one another prior to image processing. This misregistration problem is less likely to be a problem if an electro-optic filter is used to select the wavelength, rather than the traditional narrow band filters.

The proposed method using three wavelength linear images provides the best detectability of blood; however, the two wavelength ratio processing and the subtracted nonlinear images can provide adequate detection of blood under some circumstances, and these use hardware and software that are more readily available and lower cost, particularly if 8-bit image processing is used. The use of 16-bit imaging does improve the image correction method slightly compared to 8-bit processing, but given the variability of the camera pixels and most substrates the difference does not seem to be significant for many cases. The subtraction of the non-linear images does not provide as good results as the ratioing of the linear images. If the non-linear images were accurately logarithmic in light intensity the two treatments should be identical, so that the difference is likely to be due to differences from an exact logarithmic transformation combined with loss of intensity difference detail at the higher brightness levels.

It should be stressed that all the images presented in this paper have not had any image—altering filters applied and have had no individual pixels or groups of pixels treated differently from the whole image. The whole process is based on the mathematical

treatment of the whole image consistent with standard analyses of absorbance or reflectance. The method also has general precedent in geographic and astronomical image processing, as discussed in the opening section of the paper. The adaptation to include different exposure times for images is new, but the derivation provided in this paper justifies this adaptation under the conditions specified. If different exposure times were not used (as is the case with other imaging applications) the system would need to be standardized with a known neutral grey under the exact illumination conditions to be used and (at least for our system) the 395 nm image would be very underexposed (and therefore very noisy) due to the reduced light throughput at this wavelength compared to 435 nm. Therefore the use of different exposure times is an important factor in the successful application of this technique.

The technique has been described with relatively stringent conditions in order for Eq 10 (the ratioing of images) to be valid. This was done to demonstrate that the technique has a valid scientific basis and can even be used in a quantitative manner under certain controlled conditions. In operation where the detection of blood staining is of more interest than quantitation the conditions can be relaxed slightly, in particular, the images can be slightly differently exposed since the contrast adjustment will adapt for small differences in intensities between the images. Furthermore, as noted earlier, the substrate can often be used rather than a neutral greyscale to balance the relative exposures of the photographs taken at different wavelengths since even though the absorbance of the substrate will vary with wavelength it does not typically change by a large amount over a 40 nm range. In conclusion, the technique we describe allows for increased detection of potential bloodstains on patterned and non-uniformly lit substrates and can therefore provide a valuable adjunct to the traditional photographic visualization techniques used by the forensic scientist or police technician. It is, of course, still necessary to confirm that any pattern detected by this method is indeed blood using any of the standard forensic tests.

Acknowledgments

The authors thank Dr. D. Elliot and F. Matheson of ESR Ltd. for helpful discussions and for providing test clothing items. This research was supported by a grant from the University of Auckland. Some of this study was performed by J. Wagner as part of his M.Sc. in Forensic Science at the University of Auckland.

References

1. McDonald JA. Close-up and macro photography for evidence technicians. Arlington Heights: PHOTOTEXT Books; 1992.
2. Redsicker DR. The practical methodology of forensic photography. Boca Raton: CRC Press; 2001.
3. Blitzer HL, Jacobia J. Forensic digital imaging and photography. San Diego: Academic Press; 2002.
4. Russ JC. Forensic uses of digital imaging. Boca Raton: CRC Press; 2001.
5. Grady DP. Using Adobe Photoshop's channel mixer as an evidence enhancement tool. J Forensic Ident 2001;51:378–84.
6. Menzel ER. Fingerprint detection with lasers. New York: Marcel Dekker, Inc.; 1999.
7. Stoilovic M. Detection of semen and blood stains using Polilight as a light source. Forensic Sci Int 1991;51:289–96.
8. Harboe M. A method for determination of hemoglobin in plasma by near-ultraviolet spectrophotometry. Scand J Clin Lab Investig 1959;11:66–70.
9. Jensen SB, Oliver RWA. A simplified general proof of the Allen correction equation and some comments concerning its applicability to the colorimetric analysis of oestriol. Clinica Chimica Acta 1973;44:443–8.
10. Wians FH, Miller CL, Heald JI, Clark H. Evaluation of a direct spectrophotometric procedure for quantitating plasma hemoglobin. Laboratory Medicine 1988;19:151–5.
11. Wong SS, Schenkel OJ. Quantification of plasma hemoglobin in the presence of bilirubin with Bilirubin Oxidase. Ann Clin Lab Sci 1995;25: 247–52.
12. Clark RN, Roush TL. Reflectance spectroscopy: quantitative analysis techniques for remote sensing applications. J Geophys Res 1984;89: 6329–40.
13. Curran PJ, Dungan JL, Peterson DL. Estimating the foliar biochemical concentration of leaves with reflectance spectrometry. Remote Sens Environ 2001;76:349–59.
14. Kokaly RF, Clark RN. Spectroscopic determination of leaf biochemistry using band-depth analysis of absorption features and stepwise multiple linear regression. Remote Sens Environ 1999;67:267–87.
15. Profio AE, Balchum OJ, Carstens F. Digital background subtraction for fluorescence imaging. Med Phys 1986;13:717–21.
16. Tanhuanpaa K, Virtanen J, Somerharju P. Fluorescence imaging of pyrene-labeled lipids in living cells. Biochim Biophys Acta 2000;1497: 308–20.
17. Billinton N, Knight AW. Seeing the wood through the trees: a review of techniques for distinguishing green fluorescent protein from endogenous autofluorescence. Anal Biochem 2001;291:175–97.
18. Ghauch A, Turnar C, Fachinger C, Rima J, Charef A, Suptil J, et al. Use of diffuse reflectance spectrometry in spot test reactions for quantitative determination of cations in water. Chemosphere 2000;40:1327–33.
19. Tubino M, Rossi AV, de Magalhaes MEA. Quantitative spot tests of Fe(III), Cr(VI) and Ni(II) by reflectance measurements. Anal Lett 1997;30:271–82.
20. Berns RS. Principles of color technology. New York: Wiley & Sons, Inc.; 2000.
21. Wendlandt WW, Hecht HG. Reflectance spectroscopy. New York: J. Wiley & Sons; 1966.

Additional information and reprint requests:
Gordon M. Miskelly, Ph.D.
Forensic Science Programme
Department of Chemistry
The University of Auckland
Private Bag 92019
Auckland
New Zealand
E-mail: g.miskelly@auckland.ac.nz